

# Regulation of synaptic connectivity in schizophrenia by mutual neuron-microglia interaction

Ricarda Breitmeyer

Sabrina Vogel

Johanna Heider

Richard Wüst

Anna-Lena Keller

Anna Binner

Julia Fitzgerald

Department of Neurodegenerative Diseases, Centre of Neurology and Hertie Institute for Clinical Brain Research, University of Tübingen.

Andreas Fallgatter

Hansjürgen Volkmer (✉ [volkmer@nmi.de](mailto:volkmer@nmi.de))

NMI an der Universität <https://orcid.org/0000-0002-3867-0603>

---

## Article

### Keywords:

**Posted Date:** July 13th, 2022

**DOI:** <https://doi.org/10.21203/rs.3.rs-1792046/v1>

**License:**   This work is licensed under a Creative Commons Attribution 4.0 International License.

[Read Full License](#)

---

**Version of Record:** A version of this preprint was published at Communications Biology on April 29th, 2023. See the published version at <https://doi.org/10.1038/s42003-023-04852-9>.

# Abstract

The examination of post-mortem brain tissue suggests synaptic loss as a central pathological hallmark of schizophrenia. Synaptic loss has been shown to be related to increased inflammation in the central nervous system. Aberrant activation of microglia, the immune cells of the human brain, may account for neuronal damage in schizophrenia. Induced pluripotent stem cells represent a promising tool for studying neuropsychiatric disease mechanisms. A recent challenge has been the development of protocols to derive microglia as well as neurons from schizophrenia patient-derived stem cells to better understand the mechanistic contribution of neuroinflammation to the disease. To address this, we present a co-culture model of neurons and microglia, both of human origin to show increased susceptibility of neurons to microglia-like cells derived from schizophrenia patients. Analysis of IBA-1 expression, NFκB signaling, transcription of inflammasome-related genes, and caspase-1 activation shows that enhanced, intrinsic inflammasome activation in patient-derived microglia exacerbates neuronal deficits such as synaptic loss in schizophrenia. Anti-inflammatory pretreatment of microglia with minocycline specifically rescued aberrant synapse loss in schizophrenia and reduced microglial activation. These findings open up possibilities for further research in larger cohorts, focused clinical work and longitudinal studies that could facilitate earlier therapeutic intervention.

## Introduction

Schizophrenia (SCZ) is a complex and highly heterogeneous mental disorder characterized by severe disabling social and clinical impairments. The broad range of individual psychotic symptoms includes hallucinations, delusions, apathy and withdrawal, as well as cognitive deficits. Diverse symptoms in combination with a huge variability between individual patients complicates the understanding of underlying biological causes and hampers the development of novel therapeutics. So far, antipsychotic drug application aims to reduce symptom severity and improve quality of life, but there is currently no cure available. Genetic predispositions, prenatal stress or social and environmental factors have been suggested to contribute to disease pathology. A majority of research focuses on altered neurobiological function, such as deregulated neurotransmitter release and aberrant neuronal activity. More recently, epidemiological studies and genome-wide association studies suggested a link between SCZ and prenatal infection, systemic inflammation and immune system dysfunction<sup>1-5</sup>.

Microglia, the immune cells of the central nervous system, emerge as key regulators of early neurodevelopment and synaptic plasticity, while governing neuroimmunological responses. In SCZ, aberrant neuroinflammation mediated by reactive microglia may account for synaptic and neuronal pathologies. PET imaging revealed elevated microglial activation in SCZ patients, while peripheral cytokine levels were increased<sup>6-8</sup>. Likewise, post-mortem tissue analysis and PET imaging of patients repeatedly showed decreased cortical volume and reduced synaptic density<sup>9-12</sup>. These findings strengthened the hypothesis that an increased inflammatory state of microglia is responsible for the observed loss of neuronal connectivity in SCZ. So far, it is not understood how microglial activation in SCZ contributes to the underlying pathology.

The prevailing view of SCZ etiology has relied on mainly peripheral markers, imaging and post mortem studies in patient fibroblasts. Recent advances in human induced pluripotent stem cell (iPSC) models provide a valuable tool for studying disease-relevant and patient-specific mechanisms of SCZ in neurons<sup>13-15</sup>. Examination of the interaction of neurons and microglia in iPSC-derived models remained a challenge in the field, but a complete human model comprising both cell types is greatly needed for SCZ research. So far, microglia-like cells were either generated from blood-derived monocytes and exposed to acellular synaptosome preparations, or human interneurons were co-cultivated with murine microglial cell lines<sup>16,17</sup>.

This prompted us to differentiate neurons and microglial cells from iPSCs of the same donor with its genetic background to setup co-culture models that allow the study of neuron-microglia interactions for the understanding of inflammatory processes in SCZ. Here, we made use of a collection of previously described iPS cell lines from patients with schizophrenia to establish a fast microglia differentiation protocol<sup>18</sup>. We show that SCZ microglia display an elevated activation state as compared to healthy controls that is linked to increased TNF $\alpha$  secretion and NF $\kappa$ B signaling as well as to enhanced inflammasome activity. Likewise, microglia-like cells were combined with NGN2-induced neurons for an iPSC-derived co-culture that allows for the analysis of neuronal and microglial phenotypes in SCZ via direct cell-cell interactions. When co-cultured with SCZ neurons, SCZ microglia exacerbate the intrinsic deficit of SCZ neurons to form synapses, while SCZ neurons enhance microglial activation. Importantly, anti-inflammatory pretreatment of microglial cells specifically rescues SCZ-associated synaptic loss while having no impact on healthy controls.

## Material And Methods

The methods were performed in accordance with relevant guidelines and regulations and approved by the Ethics Committee of the University Hospital and Faculty of Medicine Tuebingen. We confirm that participants provided a written informed consent to take part in the study. Inclusion and exclusion criteria for the selection of patients diagnosed with schizophrenia are described in Supplementary Table 2. iPSCs were generated and fully characterized as described elsewhere<sup>18,19</sup>.

## Microglia Differentiation and Co-Culture with NGN2-Neurons

For microglia generation, we modified a previously published protocol for the differentiation of iPSC into monocytes and macrophages<sup>22</sup>. The stepwise differentiation is driven by the sequential induction of mesoderm towards CD45<sup>+</sup> hematopoietic stem cells for nine days. For microglial differentiation and maturation, the necessary growth factors were adapted to ensure optimal microglial differentiation. In this study, CD45<sup>+</sup> precursor cells were exposed to 100 ng/ml of IL-34, 50 ng/ml of TGF $\beta$ 1 and 25 ng/ml of GM-CSF (all from Peprotech, USA) for ten days. TGF $\beta$ 1 has previously been shown to comprise a crucial brain-derived signal for microglial specification<sup>23</sup>. For details, please see supplementary

information. Microglia were routinely characterized regarding expression of key markers like IBA1, SPI1 and TMEM119. Functionality was proven by active uptake of pHrodo-labelled bacteria and response to LPS as a pro-inflammatory stimulus. Microglia identity was confirmed by RNA sequencing. Transcriptome analysis and bioinformatical evaluation was performed by CeGaT GmbH (Germany) as previously described <sup>10</sup>.

Neurons were differentiated using a previously published two-step protocol <sup>20,21</sup>. Briefly, iPSCs were predifferentiated into neural progenitor cells (NPCs) using the STEMdiff™ Neuronal Induction Kit (STEMCELL Technologies, Canada). Quality of NPCs was confirmed by regular immunocytochemical stainings for PAX6, Nestin or SOX1. Subsequent neuronal differentiation was achieved by lentiviral overexpression of human Neurogenin 2. Neuronal networks stained positive for neuronal markers like MAP2 or  $\beta$ -III-tubulin or synaptic markers like Synapsin1 or VGLUT1. For further details, see supplementary information.

After separate induction of neuronal and microglial differentiation for 16 days, microglial cells were seeded to NGN2-neurons in a ratio of 1:5 as outlined in Fig. 5B. In case of microglial pretreatment, microglia were stimulated using 100 ng/ml of LPS (Sigma-Aldrich, USA), 10  $\mu$ M of Minocycline (STEMCELL Technologies, Canada) or 0.1% DMSO (Carl Roth, Germany) as vehicle control for one hour at 37°C. Microglia were washed once with DPBS and seeded onto neuronal networks in microglia culture medium. Microglia and neurons were co-cultivated for 72 hours. A detailed description is provided in supplementary information.

## Additional experiments

For details regarding lentiviral production, p65 expression, caspase-1 assay, ELISA, flow cytometry, immunocytochemistry and confocal imaging, please see supplementary information.

## Statistics

Statistical analysis was performed using GraphPad Prism 9.2.0 (GraphPad Software Inc.). For non-Gaussian distribution in pairwise comparisons, the unpaired Mann-Whitney U test was performed and for group comparisons, Kruskal-Wallis test with Dunn's post-hoc multiple comparisons test was used. The type of statistical test used is reported in the figure legends or main text. P-values were assigned as follows: \* =  $p < 0.05$ , \*\* =  $p < 0.01$ , \*\*\* =  $p < 0.001$ .

## Results

### Differentiation of microglial cells from iPSC

iPS cell lines from two healthy volunteers and four cell lines from four patients with SCZ were used in this study as indicated in Supplementary Table 1 <sup>18,19</sup>. Patients were diagnosed according to DSM-IV (Supplementary Table 2). Microglia were generated from iPSC by high-dose application of IL-34, TGF $\beta$ 1 and GM-CSF to optimize specification of microglia (Fig. 1A). Microglia-like cells showed ramified

processes indicative of a resting state morphology. Flow cytometry analysis of differentiating cells over 19 days revealed a dynamic downregulation of the stem cell marker SSEA-4, while hematopoietic and microglial markers CD45 and CD11b, respectively, became upregulated (Fig. 1B). Immunocytochemical analysis of microglial marker proteins including the transcription factor SPI1 as well as P2RY12 and TMEM119 confirmed a specific microglial phenotype (Fig. 1C), while immune cell and microglia-specific marker proteins SPI1, CX3CR1 or IBA1 were undetectable in the respective iPSC lines (Supplementary Fig. 1). A pH-sensitive uptake assay with *Escherichia coli*-derived bioparticles revealed phagocytic functions of differentiated microglia (Supplementary Fig. 2). For a more comprehensive analysis of microglia-like cells, we applied RNA sequencing for the comparison of iPSC with microglia-like cells (Fig. 1D). The results indicated downregulation of stem cell genes, while key microglial marker and specific transcription factor genes became upregulated. In detail, RNA sequencing identified upregulation of genes involved in chemokine or cytokine signaling, antigen processing and presentation as well as toll-like receptor signaling in differentiated microglia as compared to naïve iPSC cells (Supplementary Fig. 3). Likewise, LPS stimulation increased pro-inflammatory gene expression of NFκB1, IL-1β, TNFα as well as immune response genes such as CIITA and HLA-DBR1 (Supplementary Fig. 4). iPSC derived from healthy volunteers and patients diagnosed with schizophrenia displayed no differences in differentiation capacity, microglial cell yield (Supplementary Fig. 5), or differential expression of microglia key genes (Fig. 1E-M). In conclusion, the newly developed differentiation protocol proved to be suitable for the generation of microglia-like cells.

## **Elevation of immune-related transcripts in SCZ microglial cells**

RNA sequencing was applied to identify deregulated transcripts in SCZ. Among the upregulated genes, we found neuronatin (NNAT), glutathion S-transferase M1 (GSTM1), NLRP2, NLRP3, and TLR4 (Fig. 2A-E, Supplementary Table 3). NLRP2 and 3 as well as TLR4 are linked to NFκB signaling and inflammasome functioning<sup>24</sup>. In contrast, NLRP1 remained equally expressed in healthy control and SCZ samples (Fig. 2F). GSTM1 and NNAT were previously suggested to be involved in inflammation<sup>25,26</sup>. We also observed an increased mRNA expression of the SCZ-risk gene complement factor C4A (Fig. 2G), a further regulator of the innate immune response, which is in agreement with mRNA quantifications performed on patient samples<sup>27</sup>. C4B expression was upregulated in SCZ microglia, although statistical significance was not achieved (Fig. 2H). In summary, microglia-like cells derived from patients with SCZ showed increased expression of genes involved in inflammation.

## **Activation of iPSC-derived microglial cells in SCZ**

Next, we examined the activated state of microglial cells more closely to link the transcriptomic profiles to microglial functionalities. In support of an enhanced inflammatory state of SCZ microglia, we observed increased TNFα levels in the supernatant of SCZ microglial cells as compared to healthy control microglia (Fig. 3A). In parallel, quantitative imaging revealed upregulated IBA1 expression (Fig. 3B). Increased TNFα levels might induce NFκB signaling after binding to the TNFα receptor. Analysis of NFκB

translocation into the nucleus as a measure for NFκB activation showed increased NFκB levels in the nucleus of SCZ microglia-like cells (Fig. 3C + D, Fig. 3E for quantification). Enhanced expression of NLRP suggests a contribution of inflammasome assembly in SCZ phenotypes. Inflammasome activation is signified by caspase-1 activation<sup>28</sup>. Measurement of caspase-1 activity as a readout for inflammasome functioning revealed increased caspase-1 activation in SCZ samples in comparison to healthy controls (Fig. 3F). This finding was replicated in after stimulation with LPS. We conclude that SCZ microglia-like cells show an increased inflammatory state signified by enhanced inflammasome activity.

## **Neurons derived from SCZ-iPSCs exhibit reduced synaptic density**

For the setup of a microglia-neuron co-culture model, glutamatergic neurons were differentiated from iPSC-derived neuronal progenitor cells (NPC) by lentiviral overexpression of human Neurogenin 2 (*hNGN2*; Fig. 4A) and further co-cultivation with murine astrocytes to enhance neuronal maturation and synapse formation as published previously (Supplementary Fig. 6<sup>29</sup>). NPCs expressed their cognate marker proteins Nestin, SOX1, and PAX6 (Fig. 4B + C). Differentiated neurons elaborated MAP2-positive as well as β-III-tubulin-positive neurites (Fig. 4D + E), and showed expression of presynaptic (Synapsin 1, Synaptophysin, VGlut1) and postsynaptic (Homer) marker proteins (Fig. 4F-I). Synapse densities were subsequently calculated as the number of Synapsin 1 (SYN1)-positive spots within MAP2-positive dendritic segments (Fig. 4K + L). The analysis revealed a significant reduction of SYN1 spots in neurons derived from individual patients with SCZ. Data retrieved across experimental replicates demonstrate reproducibility and robustness (Supplementary Fig. 7). In conclusion, neurons derived from schizophrenia patients showed an intrinsic deficit in the formation or maintenance of synapses.

## **Microglia-neuron interactions have a synergistic effect on SCZ-induced neuronal deficits**

Neurons and microglia-like cells were separately differentiated from iPSC and subsequently combined in co-cultures comprising all four combinations of healthy/SCZ microglia and healthy/SCZ neurons (Fig. 5A + B). After 72 hours, IBA1-positive microglia cultivated on MAP2-positive neuronal networks displayed a ramified morphology (Fig. 5C, higher magnification Fig. 5D). For the evaluation of reciprocal interactions between neurons and microglia in SCZ, we examined synapse densities of neuronal dendrites (Fig. 5E), the phagocytosis of presynaptic material by microglia (Fig. 5G), and the activation state of microglia (Fig. 5H).

First, presynaptic Synapsin1 (SYN1) spot densities in neurons localized at MAP2-positive dendrites were determined as an approximation for the impact of microglia on neuronal synapse numbers (Fig. 5E). The mere addition of microglia of any kind significantly reduced the density of SYN1 spots as compared to a pure neuronal culture (Supplementary Fig. 8), suggesting baseline synapse elimination by microglia-like cells. Addition of SCZ microglia (mgSCZ) to CTR neurons significantly reduced the number of SYN1 spots in comparison to healthy control microglia (mgCTR, Fig. 5E, Supplementary Fig. 9). Likewise,

exposure of SCZ microglia to SCZ neurons exacerbated the intrinsic synaptic deficits of SCZ neurons. In the presence of CTR microglia, synapse densities of SCZ neurons were significantly decreased in comparison to CTR neurons. This observation may either reflect the intrinsic deficit of SCZ neurons to form synapses or may alternatively indicate an increased susceptibility of SCZ neurons towards an extrinsic microglial impact. The stepwise decrease in synapse numbers from the control situation (CTR neurons/CTR microglia) with an intermediate effect for the mixed combinations (SCZ neurons and CTR microglia or CTR neurons and SCZ microglia) towards a maximal synapse loss in co-cultures of SCZ neurons and SCZ microglia suggests that synaptic depletion is a synergistic result of deficient synapse formation in SCZ neurons and aberrant synapse elimination by SCZ microglia.

Due to the phagocytic activity of microglial cells, we were prompted to investigate whether the synapse loss that occurs on dendrites is due to increased uptake of synaptic material by microglia. We therefore analyzed the uptake of presynaptic material into IBA1-positive microglia co-cultured with neurons (Fig. 5F + G). Uptake of synaptic material was detected and quantified as outlined in Supplementary Fig. 10. Immunocytochemistry revealed co-localization of SYN1-positive material and LAMP1-positive lysosomes suggesting active uptake of presynapses and thus synaptic pruning by microglia-like cells (Fig. 5F). Quantification of synapse uptake (Fig. 5G) revealed a complementary effect of increasing synaptic uptake to decreasing synapse density (Fig. 5E) indicating active elimination of synapses by microglia. Synapse uptake by SCZ microglia co-cultured with CTR or SCZ neurons was significantly increased as compared to CTR microglia, which is in line with an enhanced microglial activation state in SCZ. CTR microglia phagocytosed more presynaptic material from SCZ neurons than from CTR neurons, providing further evidence for increased susceptibility of SCZ neurons to a microglial impact beside the intrinsic deficits of SCZ neurons to form synapses. To understand the impact of soluble factors as a mediator of microglial impact, we next asked the question whether a direct microglia-neuron cell-cell contact was required for synapse removal. Supernatants from neuron-microglia co-cultures of all combinations were collected and applied to pure neuronal CTR and SCZ cultures. While SYN1 density was generally reduced in SCZ neurons, no impact of cell culture supernatants of any kind was observed (Supplementary Fig. 11) suggesting that cell-cell contacts rather than soluble factors are mediating active synapse elimination by microglia.

We next examined the activation state of microglia in neuron-microglia co-cultures. IBA1 expression was quantified in all combinations of co-cultures from CTR and SCZ individuals (Fig. 5H). IBA1 expression was increased in SCZ microglia as compared to CTR microglia after co-culture on CTR neurons, indicating that SCZ microglia are intrinsically activated. CTR microglia exposed to SCZ neurons showed an increased activation state compared to CTR microglia that were co-cultured with CTR neurons. This suggests a direct impact of SCZ neurons on microglia resulting in increased levels of microglial activation. This finding was replicated after incubation of SCZ microglia with SCZ neurons and in comparison to CTR neurons. Altogether, our findings suggest intrinsic enhanced activation of SCZ microglia that becomes worsened by extrinsic signals supplied by SCZ neurons.

# Anti-inflammatory pretreatment of microglia rescues schizophrenia phenotypes

Next we asked whether modulation of microglial inflammasome functioning mitigates the observed reduction in synapse densities provoked by neuron-microglia interactions. The tetracycline antibiotic minocycline activates Nrf2 and thereby reduces reactive oxygen species-induced inflammasome activation<sup>30</sup>. We therefore pretreated microglial cells with minocycline prior to exposure to neurons in the co-culture model and compared CTR microglia/CTR neuron combinations with SCZ microglia/SCZ neurons (Fig. 6, example images in Fig. 6A). Pretreatment of microglia with minocycline did not modulate neuronal synapse densities in the control situation (Fig. 6B). However, synapse densities were specifically increased in the SCZ co-cultures (Fig. 6C). Quantification of microglial synapse uptake revealed no impact of minocycline in the control setup while in SCZ co-cultures synapse uptake was significantly decreased (Fig. 6D + E). Accordingly, minocycline reduced microglial activation as measured by IBA1 expression only in SCZ co-cultures, while having no effect on CTR microglia further underlining the selective impact of minocycline on SCZ samples (Fig. 6F + G). Interestingly, LPS pretreatment selectively reduced the density of synapses in CTR neurons (Fig. 6B), and increased uptake of synaptic material in CTR microglia (Fig. 6D), while no effects were observed in SCZ co-cultures (Fig. 6C + E). In contrast, LPS treatment increased IBA1 expression and microglial activation under CTR and SCZ conditions (Fig. 6F + G). Further combinations of control and patient-derived neuron-microglia co-cultures are shown in Supplementary Fig. 12. In conclusion, minocycline rescued the SCZ phenotype regarding microglial activation, synapse uptake and neuronal synapse densities. LPS enhanced microglial activation as suggested by increased IBA1 expression. However, this effect does not precipitate into increased loss of neuronal synapses or increased microglial uptake of synaptic material in SCZ samples, suggesting a saturating effect of SCZ-related mechanisms.

## Discussion

Patient-derived and disease-specific cellular models offer great potential to better understand the ambivalent communication of key cellular players in neurodevelopmental disorders with a huge heterogeneity and divergent molecular causes. Here, we present an iPSC-based co-culture model comprising human neurons and microglia to analyze neuro-immune interactions in SCZ samples. We demonstrate that both neuronal and microglial features contribute to excessive elimination of presynaptic terminals. Intrinsic properties of SCZ patient-derived neurons lead to decreased synapse densities, while SCZ microglia showed an enhanced activation state of microglia, increased TNF $\alpha$  secretion and elevated NF $\kappa$ B signaling compared to healthy microglia. This was accompanied by an upregulation of inflammasome genes NLRP2 and NLRP3, which are targets of NF $\kappa$ B signaling and are involved in the activation of the inflammasome by caspase-1.

Increased IBA1 immunoreactivity indicates an enhanced activated state of SCZ microglia, which correlates with increased TNF $\alpha$  secretion. In this line, peripheral TNF $\alpha$  is increased in SCZ as found in a

meta-analysis of patients with schizophrenia<sup>31</sup>. TNF $\alpha$  may bind to the TNF $\alpha$  receptor and subsequently induce NF $\kappa$ B signaling. The TNF $\alpha$  gene by itself represents a downstream target of NF $\kappa$ B and may therefore serve for sustained maintenance of an activated microglial state<sup>32</sup>. Our expression analysis also implies that other receptors such as TLR4 become upregulated in SCZ microglia, which may further exacerbate NF $\kappa$ B signaling<sup>33</sup>.

Our observations strongly argue for a contribution of the inflammasome system in SCZ as documented by increased NF $\kappa$ B signaling linked with upregulated NLRP2/3, and enhanced caspase-1 activity. Inflammasome functioning relies on two consecutive steps including priming and activation that finally activate caspase-1 for cleavage and secretion of IL-1 $\beta$ <sup>28</sup>. The priming step includes activation of NF $\kappa$ B and upregulation of inflammasome genes. We observed induction of NLRP2 and NLRP3 transcription both of which represent central components of the inflammasome<sup>34,35</sup>. NLRPs subsequently serve as sensors for cellular stress for inflammasome activation<sup>28</sup>. Mitochondrial dysfunction and production of reactive oxygen species serve as a potential inflammasome activator and are discussed as an important mechanism contributing to SCZ<sup>36-38</sup>. Interestingly, minocycline was shown to inhibit reactive oxygen species-dependent inflammasome activation through stabilization of the antioxidant Nrf2<sup>30,39</sup>. Here, we report that minocycline pretreatment of microglial cells rescued both the activation state of SCZ microglia and additionally preserved neuronal synapses in the co-culture model. This observation therefore supports the hypothesis that inflammasomes are crucially involved in microglia-dependent synaptic loss in SCZ.

A final step includes the activation of the inflammasome component caspase-1, which is required for cleavage of pro-IL-1 $\beta$  and subsequent release of IL-1 $\beta$ . Increased levels of IL-1 $\beta$  were found in patients with SCZ<sup>40</sup>. In accordance with our observation that synaptic densities are reduced in neurons upon exposure to SCZ microglia, IL-1 $\beta$  was suggested to inhibit BDNF signaling, a mechanism required for morphological and functional synaptic plasticity<sup>41</sup>. In accordance with an impact on synapses in particular of the prefrontal cortex, minocycline ameliorates negative symptoms in patients with SCZ and reduces IL-1 $\beta$  levels in parallel<sup>42</sup>. It is of note that minocycline selectively improved SCZ phenotypes and did neither modulate synapse densities, nor SYN1 uptake or IBA1 expression in microglia of control samples, suggesting a specific effect on SCZ samples not found with healthy controls. Accordingly, a comparable effect of minocycline treatment was also described in a meta-analysis of preclinical studies performed using animal models for depression. Minocycline treatment was only effective with animals that have experienced severe stressful situations before assessment of depressive states, while no effects were observed in testing naïve animals in an otherwise healthy state<sup>43</sup>.

To conclude, deficient synapse formation in iPSC-derived models of SCZ neurons has been documented by several reports<sup>13-15</sup>. In this study, we present a new, fully iPSC-based model of microglia and neurons to study neuro-immune interactions. We observe immediate effects of SCZ-derived cells onto control cells. First, we demonstrate that in comparison to control neurons, SCZ neurons induce increased microglial activation and excessive elimination of synapses. Presumably, deposition of components of

the complement system on SCZ presynaptic terminals and interaction with microglial complement systems may represent one mechanism to explain increased susceptibility and concomitant aberrant synaptic pruning<sup>44</sup>. In line with this, we have observed increased expression of complement factor C4 in SCZ microglial cells. Second, we observe increased microglial activation after co-culture and aberrant synapse elimination of control or SCZ neurons by SCZ microglia compared to control microglia with a specific susceptibility of SCZ microglia to anti-inflammatory minocycline treatment. We cannot rule out that minocycline treatment of neurons would also rescue synaptic density in SCZ samples. Microglia were exclusively pretreated with minocycline to analyze specific immunological properties of SCZ microglia *in vitro*. Our results are in agreement with previous studies stating that increased levels of microglia activation were found in the brains of SCZ patients<sup>8</sup>. We provide evidence that deregulated inflammasome activation may represent a further potential mechanism contributing to excessive synapse loss in SCZ.

Although differentiation of microglia and neurons within 19 days and a co-culture of three days is not able to fully represent aberrant neurodevelopment and neuro-immune interaction evolving over several years in human patients, our model overcomes the need for non-human co-culture models and retains patient-specific phenotypes. Here we recapitulate SCZ features of reduced synapse density and increased microglial activation as previously visualized by PET imaging, in post mortem studies or rodent models<sup>45,46</sup>. It will be interesting in the future, to additionally test minocycline in microglia-neuron co-culture models derived from larger cohorts of iPSCs with different genetic backgrounds and in unaffected siblings of SCZ patients.

In summary, our iPSC-derived and patient-specific co-culture system offers the opportunity to study neuron-microglia interactions in SCZ in more detail. The specific effect of minocycline on SCZ microglia represents a promising approach for adjunctive therapy to antipsychotic treatment and may be helpful for future drug development.

## Declarations

## Acknowledgements

This work received financial support from the State of Baden-Wuerttemberg (grant no. AZ 35-4223.10/8), the German Federal Ministry of Education and Research (grant no. 01EK2101A), and the EUREKA initiative Eurostars (E! 7675). We appreciate technical assistance of Roswitha Fischer and Sibylle Glock. We are grateful to Frank Weise for helpful discussion.

## Author contributions

R.B. and H.V. designed experiments. R.B., S.V., J.H., R.W., A.-L. K., and A.B. performed experiments. R.B. established protocols and conducted immunocytochemical analyses, cytokine measurements, and

caspase-1 assays. J.H., S.V., A.-L. K., and A.B. contributed with iPSC maintenance and differentiation. R.W. was involved in clinical diagnosis. R.B., J.C.F., A.J.F., and H.V. wrote the manuscript.

## Competing interests

The authors declare no competing interests.

## References

1. Stefansson H, Ophoff RA, Steinberg S, Andreassen OA, Cichon S, Rujescu D *et al*. Common variants conferring risk of schizophrenia. *Nature* 2009; **460**(7256): 744-747.
2. Brown AS, Derkits EJ. Prenatal infection and schizophrenia: a review of epidemiologic and translational studies. *Am J Psychiatry* 2010; **167**(3): 261-280.
3. Khandaker GM, Zimbron J, Dalman C, Lewis G, Jones PB. Childhood infection and adult schizophrenia: a meta-analysis of population-based studies. *Schizophr Res* 2012; **139**(1-3): 161-168.
4. Schizophrenia Working Group of the Psychiatric Genomics C. Biological insights from 108 schizophrenia-associated genetic loci. *Nature* 2014; **511**(7510): 421-427.
5. Andreassen OA, Harbo HF, Wang Y, Thompson WK, Schork AJ, Mattingsdal M *et al*. Genetic pleiotropy between multiple sclerosis and schizophrenia but not bipolar disorder: differential involvement of immune-related gene loci. *Mol Psychiatry* 2015; **20**(2): 207-214.
6. Goldsmith DR, Rapaport MH, Miller BJ. A meta-analysis of blood cytokine network alterations in psychiatric patients: comparisons between schizophrenia, bipolar disorder and depression. *Mol Psychiatry* 2016; **21**(12): 1696-1709.
7. Fillman SG, Weickert TW, Lenroot RK, Catts SV, Bruggemann JM, Catts VS *et al*. Elevated peripheral cytokines characterize a subgroup of people with schizophrenia displaying poor verbal fluency and reduced Broca's area volume. *Mol Psychiatry* 2016; **21**(8): 1090-1098.
8. Trepanier MO, Hopperton KE, Mizrahi R, Mechawar N, Bazinet RP. Postmortem evidence of cerebral inflammation in schizophrenia: a systematic review. *Mol Psychiatry* 2016; **21**(8): 1009-1026.
9. Glantz LA, Lewis DA. Decreased dendritic spine density on prefrontal cortical pyramidal neurons in schizophrenia. *Arch Gen Psychiatry* 2000; **57**(1): 65-73.
10. Borgwardt SJ, McGuire PK, Aston J, Gschwandtner U, Pfluger MO, Stieglitz RD *et al*. Reductions in frontal, temporal and parietal volume associated with the onset of psychosis. *Schizophr Res* 2008; **106**(2-3): 108-114.
11. Glausier JR, Lewis DA. Dendritic spine pathology in schizophrenia. *Neuroscience* 2013; **251**: 90-107.
12. Osimo EF, Beck K, Reis Marques T, Howes OD. Synaptic loss in schizophrenia: a meta-analysis and systematic review of synaptic protein and mRNA measures. *Mol Psychiatry* 2019; **24**(4): 549-561.
13. Brennand KJ, Simone A, Jou J, Gelboin-Burkhart C, Tran N, Sangar S *et al*. Modelling schizophrenia using human induced pluripotent stem cells. *Nature* 2011; **473**(7346): 221-225.

14. Wen Z, Nguyen HN, Guo Z, Lalli MA, Wang X, Su Y *et al.* Synaptic dysregulation in a human iPS cell model of mental disorders. *Nature* 2014; **515**(7527): 414-418.
15. Grunwald LM, Stock R, Haag K, Buckenmaier S, Eberle MC, Wildgruber D *et al.* Comparative characterization of human induced pluripotent stem cells (hiPSC) derived from patients with schizophrenia and autism. *Transl Psychiatry* 2019; **9**(1): 179.
16. Sellgren CM, Gracias J, Watmuff B, Biag JD, Thanos JM, Whittredge PB *et al.* Increased synapse elimination by microglia in schizophrenia patient-derived models of synaptic pruning. *Nat Neurosci* 2019; **22**(3): 374-385.
17. Park GH, Noh H, Shao Z, Ni P, Qin Y, Liu D *et al.* Activated microglia cause metabolic disruptions in developmental cortical interneurons that persist in interneurons from individuals with schizophrenia. *Nat Neurosci* 2020; **23**(11): 1352-1364.
18. Stock R, Vogel S, Mau-Holzmann UA, Kriebel M, Wust R, Fallgatter AJ *et al.* Generation and characterization of human induced pluripotent stem cells lines from four patients diagnosed with schizophrenia and one healthy control. *Stem Cell Res* 2020; **48**: 101961.
19. Keller AL, Binner A, Breitmeyer R, Vogel S, Anderle N, Rothbauer U *et al.* Generation and characterization of the human induced pluripotent stem cell line NMli010-A from peripheral blood mononuclear cells of a healthy 49-year old male individual. *Stem Cell Res* 2021; **54**: 102427.
20. Zhang Y, Pak C, Han Y, Ahlenius H, Zhang Z, Chanda S *et al.* Rapid single-step induction of functional neurons from human pluripotent stem cells. *Neuron* 2013; **78**(5): 785-798.
21. Ho SM, Hartley BJ, Tcw J, Beaumont M, Stafford K, Slesinger PA *et al.* Rapid Ngn2-induction of excitatory neurons from hiPSC-derived neural progenitor cells. *Methods* 2016; **101**: 113-124.
22. Cao X, van den Hil FE, Mummery CL, Orlova VV. Generation and Functional Characterization of Monocytes and Macrophages Derived from Human Induced Pluripotent Stem Cells. *Curr Protoc Stem Cell Biol* 2020; **52**(1): e108.
23. Butovsky O, Jedrychowski MP, Moore CS, Cialic R, Lanser AJ, Gabriely G *et al.* Identification of a unique TGF-beta-dependent molecular and functional signature in microglia. *Nat Neurosci* 2014; **17**(1): 131-143.
24. de Rivero Vaccari JP, Dietrich WD, Keane RW. Activation and regulation of cellular inflammasomes: gaps in our knowledge for central nervous system injury. *J Cereb Blood Flow Metab* 2014; **34**(3): 369-375.
25. Kano SI, Choi EY, Dohi E, Agarwal S, Chang DJ, Wilson AM *et al.* Glutathione S-transferases promote proinflammatory astrocyte-microglia communication during brain inflammation. *Sci Signal* 2019; **12**(569).
26. Pitale PM, Howse W, Gorbatyuk M. Neuronatin Protein in Health and Disease. *J Cell Physiol* 2017; **232**(3): 477-481.
27. Sekar A, Bialas AR, de Rivera H, Davis A, Hammond TR, Kamitaki N *et al.* Schizophrenia risk from complex variation of complement component 4. *Nature* 2016; **530**(7589): 177-183.

28. Swanson KV, Deng M, Ting JP. The NLRP3 inflammasome: molecular activation and regulation to therapeutics. *Nat Rev Immunol* 2019; **19**(8): 477-489.
29. Schildge S, Bohrer C, Beck K, Schachtrup C. Isolation and culture of mouse cortical astrocytes. *J Vis Exp* 2013; (71).
30. Shahzad K, Bock F, Al-Dabet MM, Gadi I, Nazir S, Wang H *et al.* Stabilization of endogenous Nrf2 by minocycline protects against Nlrp3-inflammasome induced diabetic nephropathy. *Sci Rep* 2016; **6**: 34228.
31. Momtazmanesh S, Zare-Shahabadi A, Rezaei N. Cytokine Alterations in Schizophrenia: An Updated Review. *Front Psychiatry* 2019; **10**: 892.
32. Pekalski J, Zuk PJ, Kochanczyk M, Junkin M, Kellogg R, Tay S *et al.* Spontaneous NF-kappaB activation by autocrine TNFalpha signaling: a computational analysis. *PLoS One* 2013; **8**(11): e78887.
33. Kawai T, Akira S. Signaling to NF-kappaB by Toll-like receptors. *Trends Mol Med* 2007; **13**(11): 460-469.
34. Fontalba A, Gutierrez O, Fernandez-Luna JL. NLRP2, an inhibitor of the NF-kappaB pathway, is transcriptionally activated by NF-kappaB and exhibits a nonfunctional allelic variant. *J Immunol* 2007; **179**(12): 8519-8524.
35. Bauernfeind FG, Horvath G, Stutz A, Alnemri ES, MacDonald K, Speert D *et al.* Cutting edge: NF-kappaB activating pattern recognition and cytokine receptors license NLRP3 inflammasome activation by regulating NLRP3 expression. *J Immunol* 2009; **183**(2): 787-791.
36. Do KQ, Cabungcal JH, Frank A, Steullet P, Cuenod M. Redox dysregulation, neurodevelopment, and schizophrenia. *Curr Opin Neurobiol* 2009; **19**(2): 220-230.
37. Steullet P, Cabungcal JH, Monin A, Dwir D, O'Donnell P, Cuenod M *et al.* Redox dysregulation, neuroinflammation, and NMDA receptor hypofunction: A "central hub" in schizophrenia pathophysiology? *Schizophr Res* 2016; **176**(1): 41-51.
38. Cuenod M, Steullet P, Cabungcal JH, Dwir D, Khadimallah I, Klauser P *et al.* Caught in vicious circles: a perspective on dynamic feed-forward loops driving oxidative stress in schizophrenia. *Mol Psychiatry* 2021.
39. Liu X, Zhang X, Ding Y, Zhou W, Tao L, Lu P *et al.* Nuclear Factor E2-Related Factor-2 Negatively Regulates NLRP3 Inflammasome Activity by Inhibiting Reactive Oxygen Species-Induced NLRP3 Priming. *Antioxid Redox Signal* 2017; **26**(1): 28-43.
40. Bishop JR, Zhang L, Lizano P. Inflammation Subtypes and Translating Inflammation-Related Genetic Findings in Schizophrenia and Related Psychoses: A Perspective on Pathways for Treatment Stratification and Novel Therapies. *Harv Rev Psychiatry* 2022; **30**(1): 59-70.
41. Tong L, Prieto GA, Kramar EA, Smith ED, Cribbs DH, Lynch G *et al.* Brain-derived neurotrophic factor-dependent synaptic plasticity is suppressed by interleukin-1beta via p38 mitogen-activated protein kinase. *J Neurosci* 2012; **32**(49): 17714-17724.

42. Zhang L, Zheng H, Wu R, Kosten TR, Zhang XY, Zhao J. The effect of minocycline on amelioration of cognitive deficits and pro-inflammatory cytokines levels in patients with schizophrenia. *Schizophr Res* 2019; **212**: 92-98.
43. Reis DJ, Casteen EJ, Ilardi SS. The antidepressant impact of minocycline in rodents: A systematic review and meta-analysis. *Sci Rep* 2019; **9**(1): 261.
44. Stevens B, Allen NJ, Vazquez LE, Howell GR, Christopherson KS, Nouri N *et al*. The classical complement cascade mediates CNS synapse elimination. *Cell* 2007; **131**(6): 1164-1178.
45. Bloomfield PS, Selvaraj S, Veronese M, Rizzo G, Bertoldo A, Owen DR *et al*. Microglial Activity in People at Ultra High Risk of Psychosis and in Schizophrenia: An [(11)C]PBR28 PET Brain Imaging Study. *Am J Psychiatry*. 2016 Jan;**173**(1):44-52.
46. Onwordi EC, Halff EF, Whitehurst T, Mansur A, Cotel MC, Wells L *et al*. Synaptic density marker SV2A is reduced in schizophrenia patients and unaffected by antipsychotics in rats. *Nat Commun*. 2020 Jan 14;**11**(1):246.

## Figures

**Figure 1**

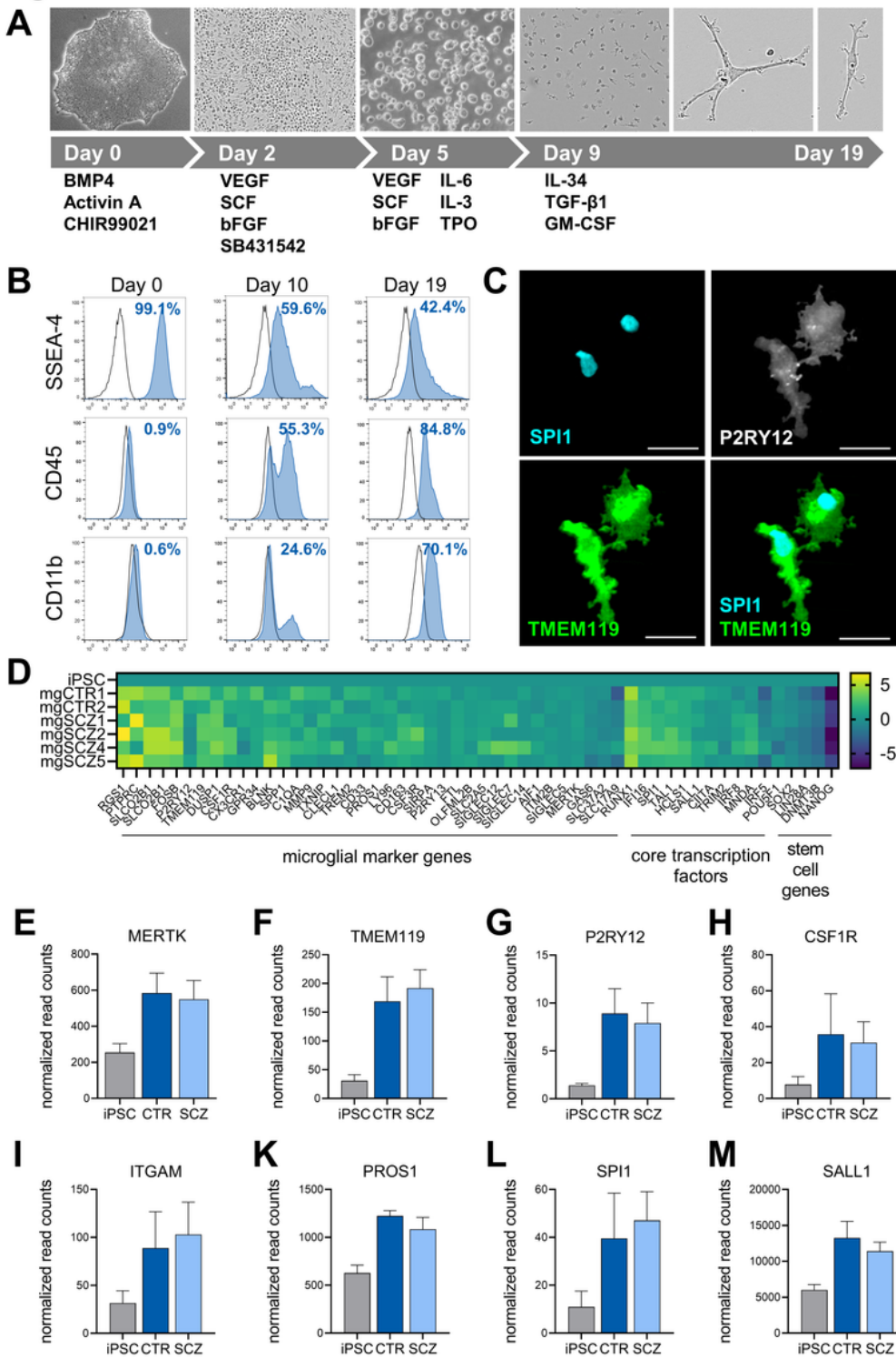


**Figure 1**

Differentiation of iPSC gives rise to microglia-like cells. (A) Schematic diagram depicting all steps of myeloid differentiation and microglial maturation from iPSC. (B) Exemplary, temporal expression of stem cell marker SSEA-4, myeloid marker CD45 and microglia marker CD11b after onset of differentiation as measured by FACS analysis. (C) Representative immunocytochemistry (63x) of day 19 microglia-like cells shows expression of microglia markers TMEM119 and P2RY12, as well as expression of the transcription

factor SPI1. Scale bar 20  $\mu$ m. (D) Heatmap displaying log<sub>2</sub> transformed expression in microglia derived from individual iPSC clones in comparison to naïve iPSC as determined by RNA sequencing. Expression of key marker genes and core transcription factors are upregulated in microglia, while stem cell genes become downregulated. (E-L) Normalized expression of microglia signature genes in CTR- and SCZ-microglia was determined by RNA sequencing. Microglial RNA was extracted from untreated, day 19 microglia derived from three independent differentiations for two control and four patient-derived lines. RNA was extracted from cells in different passages. No differences in microglia marker gene expression were detectable indicating that the differentiation protocol is equally efficient for control and patient-derived cells and the cells' capacity to differentiate is not affected in SCZ. Normalized read counts are represented as mean  $\pm$  SEM, n > 3 for each group.

## Figure 2

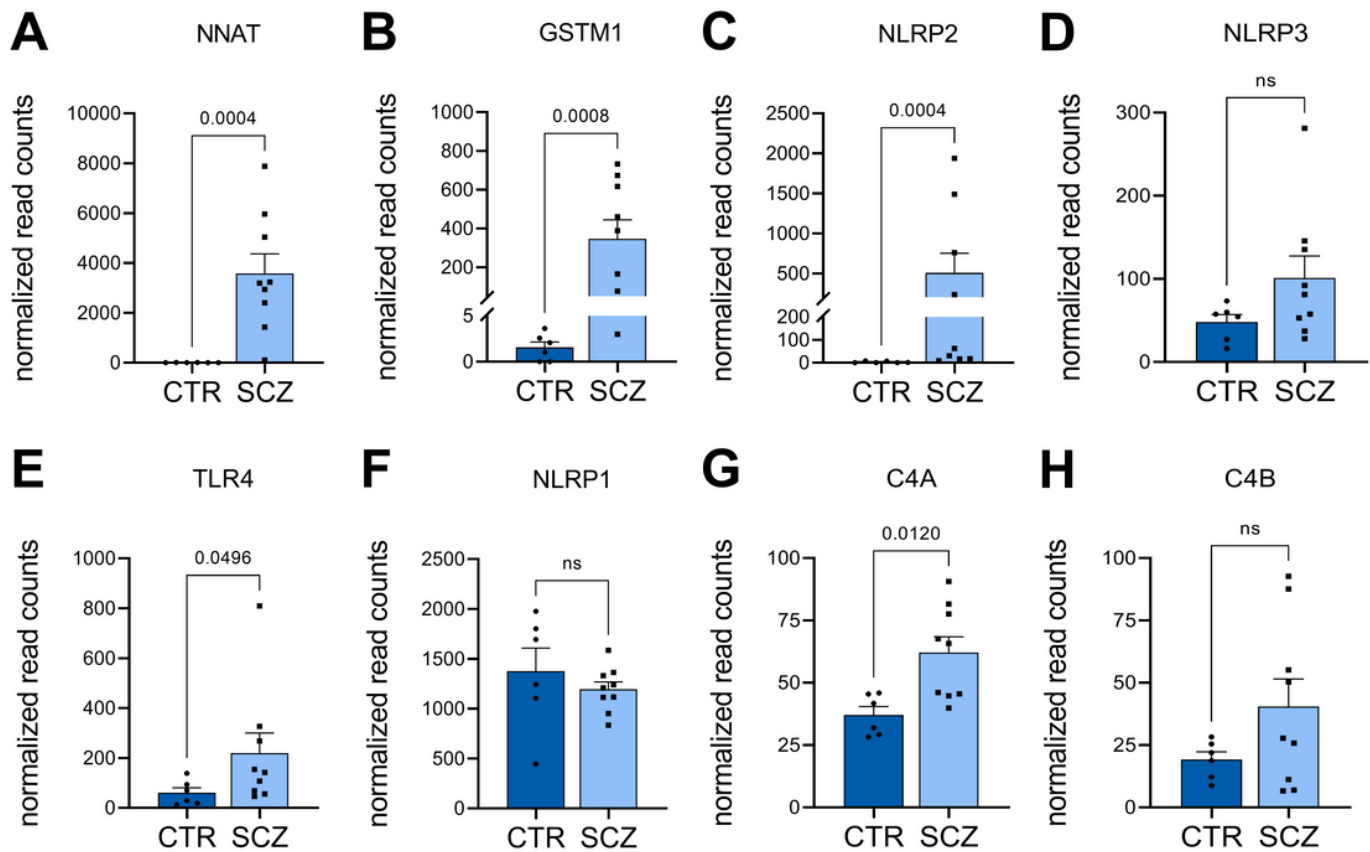


## Figure 2

Differential expression of inflammation- and complement-related genes in untreated CTR and SCZ microglia-like cells by RNA sequencing. RNA was extracted from untreated, day 19 microglia derived from three independent differentiations for two control and four patient-derived lines. Unpaired, two-tailed Mann Whitney U test was employed for pairwise comparisons, n > 6 for each individual group. Data are

represented as mean  $\pm$  SEM, ns = not significant. (A+B) RNA sequencing revealed a significant upregulation of the genes NNAT ( $p = 0.0004$ ) and GSTM1 ( $p = 0.0008$ ) in SCZ microglia compared to CTR microglia. (C+D) Quantification of NLRP2 and NLRP3 gene expression, which are involved in the activation of the inflammasome or caspase-1 activity. RNA Sequencing revealed a significant upregulation of NLRP2 in SCZ microglia ( $p = 0.0004$ ). Similarly, NLRP3 expression is slightly increased ( $p = 0.181$ ). (E) TLR4 gene expression is significantly upregulated ( $p = 0.0496$ ) in SCZ microglia. (F) NLRP1 expression is in contrast to its family members NLRP2 and NLRP3 not significantly altered in SCZ microglia. (G+H) Expression of complement and schizophrenia-associated risk gene C4A is significantly increased ( $p = 0.012$ ) in SCZ-microglia, while C4B expression is slightly but not significantly increased.

**Figure 3**

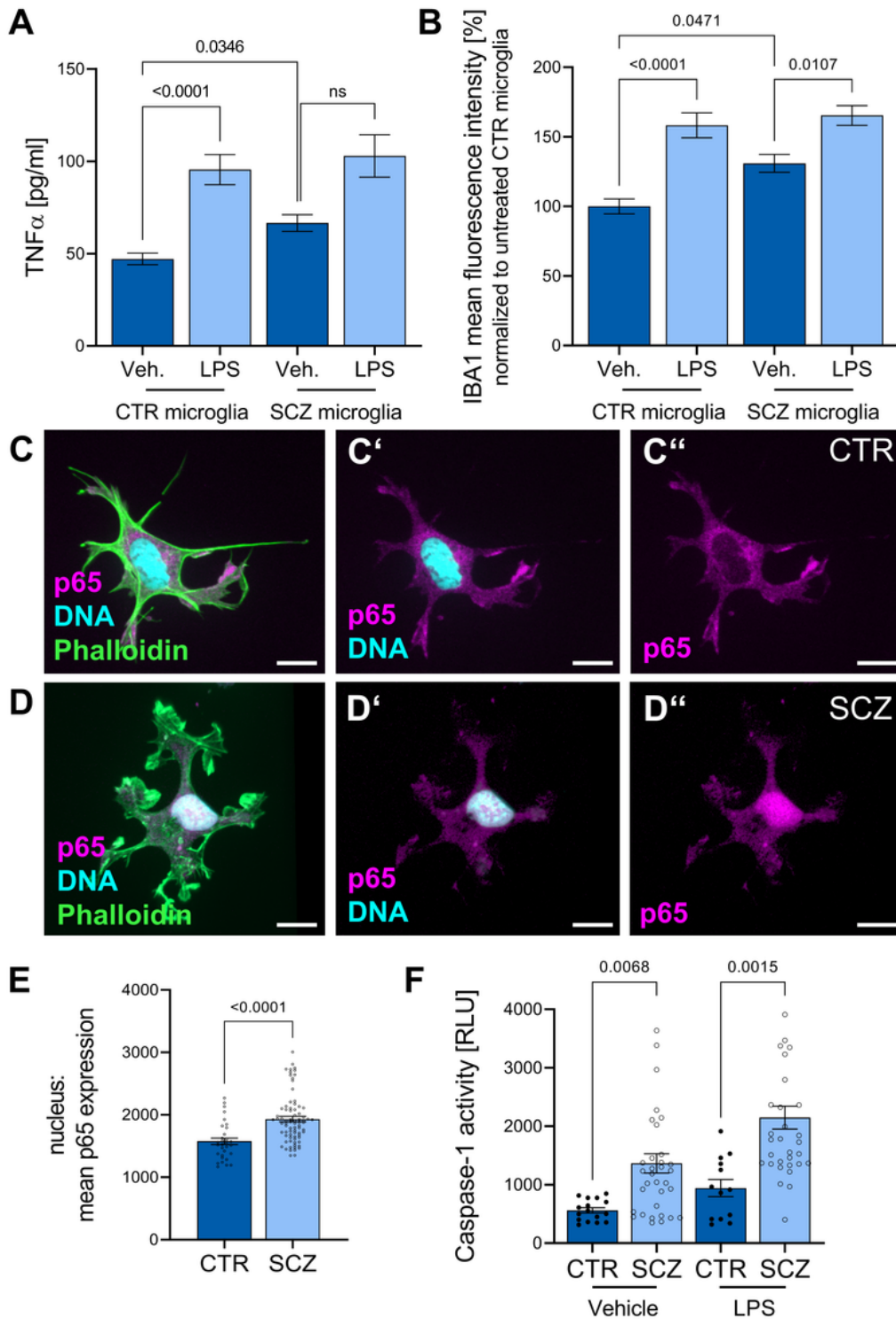


**Figure 3**

SCZ microglia show a proinflammatory phenotype in combination with significant inflammasome activation. (A) Quantification of TNF $\alpha$  release after LPS treatment (100 ng/ml) for 24 hours in comparison to vehicle-treated microglia by a sandwich enzyme-linked immunosorbent assay (ELISA). Kruskal-Wallis test with Dunn's post hoc test,  $H(3) = 30.0$ . Data are represented as mean  $\pm$  SEM from three independent experiments ( $n > 12$  for each group), ns = not significant. (B) Quantitative analysis of mean

IBA1 fluorescence intensity of CTR and SCZ microglia treated with LPS (100 ng/ml) for 24 hours as an indirect measurement for microglial activation. Kruskal-Wallis test with Dunn's post hoc test,  $H(3) = 34.6$ . Data are represented as mean  $\pm$  SEM from three independent experiments ( $n > 20$  for each group). P-values ranged from  $<0.0001$  to  $0.0471$ . (C+D) Representative immunocytochemical stainings of day 19 CTR (C) and SCZ (D) microglia taken at 63x magnification using confocal microscopy. Microglia were stained for Phalloidin, the transcription factor p65 as a subunit of the nuclear factor NF-kappa-B (NFkB) and Hoechst for nucleus visualization. (E) p65 expression within the nucleus was quantified and revealed an increased p65 expression in unstimulated SCZ microglia compared to control cells. Unpaired, two-tailed Mann Whitney U test with a p-value of  $<0.0001$ . Data are represented as mean  $\pm$  SEM from three independent experiments ( $n > 30$  for each group). (F) Caspase-1 activity was further quantified using a bioluminescent assay as a direct readout for inflammasome formation and activation. Cells were treated with 100 ng/ml LPS for 3 hours as positive control for inflammasome activation. Kruskal-Wallis test with Dunn's post hoc test,  $H(3) = 38.17$ . P-values ranged from  $0.0015$  to  $0.0068$ , indicating increased inflammasome activation in SCZ microglia. Data are represented as mean  $\pm$  SEM from three independent experiments ( $n > 12$  for each group).

**Figure 4**

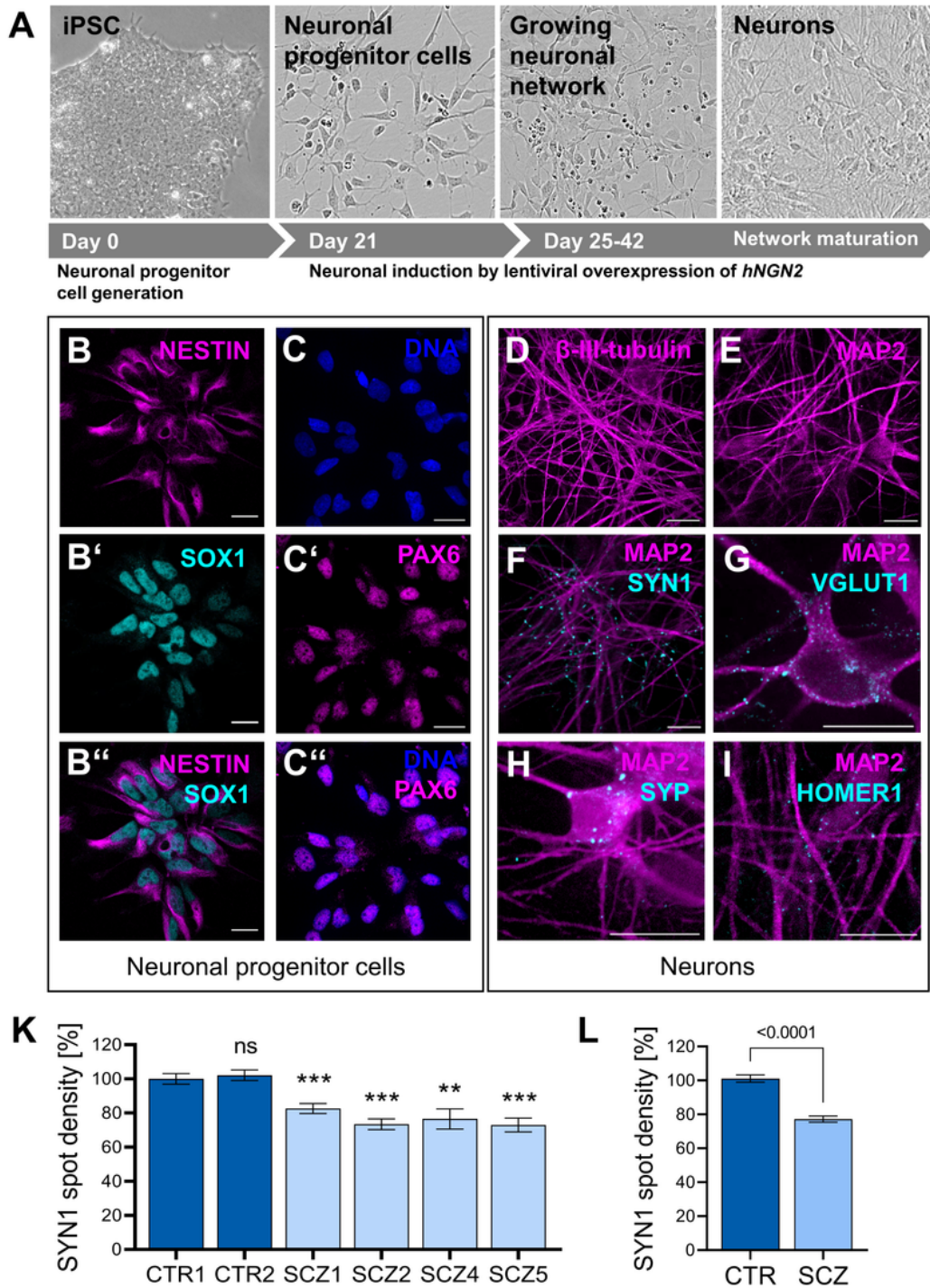


**Figure 4**

Presynaptic marker density is significantly reduced in neuronal cultures derived from schizophrenia patients. (A) Schematic overview of neuronal induction and maturation through lentiviral overexpression of hNGN2. (B+C) Representative images taken at 63x magnification using confocal microscopy and characterization of neuronal progenitor cells by immunocytochemistry with expression of standard markers such as NESTIN, SOX1 and PAX6. Scale bar 20  $\mu$ m. (D-I) Representative images taken at 63x

magnification using confocal microscopy and characterization of neuronal networks by immunocytochemical stainings for neuronal markers  $\beta$ -III-tubulin or MAP2 and presynaptic markers synapsin-1 (SYN1), vesicular glutamate transporter 1 (VGLUT1) and synaptophysin (SYP) as well as the postsynaptic marker protein HOMER1. Scale bar 20  $\mu$ m. (K) Reduced presynaptic density was quantified by analyzing the number of synapsin-1 spots detected on MAP2-positive neuronal networks. Control clone CTR1 was set as 100 %. Kruskal-Wallis test with Dunn's post hoc test,  $H(5) = 71.3$ . Data are represented as mean  $\pm$  SEM from at least five independent experiments ( $n > 80$  for each group), p-values ranged from  $<0.0001$  to  $0.0022$ , ns = not significant. (L) SYN1 density in pooled control and patient-derived neuronal cultures. Unpaired, two-tailed Mann-Whitney U test. Data are represented as mean  $\pm$  SEM ( $n = 262$  for CTR,  $n = 333$  for SCZ),  $p < 0.0001$ .

**Figure 5**

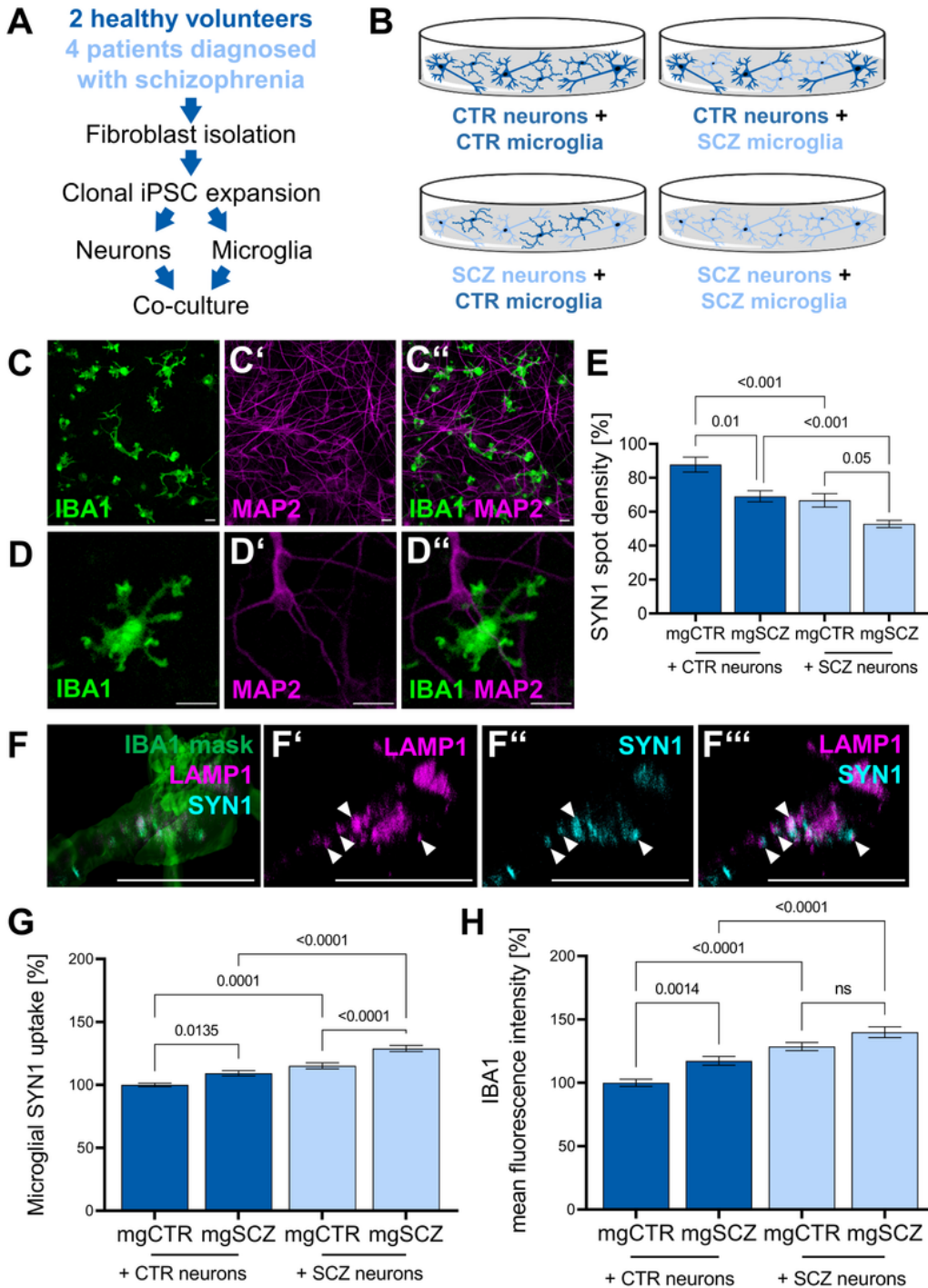


**Figure 5**

Reciprocal interplay of microglia and neurons *in vitro* reveals aberrant presynaptic uptake by SCZ microglia. (A) Design of co-culture setup comprising iPSC reprogramming from control- or patient-derived fibroblasts. iPSC are expanded and differentiated separately towards microglia or neurons. Finally, microglia and neurons are seeded into co-culture at a ratio of approximately 1:5 for 72 hours. (B) Schematic overview of the different combinations of control- or patient-derived microglia and neurons

used in this study. (C+D) Representative immunocytochemical images taken at 20x (C) or at 63x (D) magnification using confocal microscopy of IBA1 positive microglia in co-culture with MAP2 positive neurons. Scale bar 20  $\mu$ m. (E) Density of SYN1 spots was significantly reduced in SCZ microglia-neuron co-cultures. SYN1 spot densities were quantified on MAP2-positive neuronal networks and were normalized to SYN1 spot densities on CTR neurons cultivated in the absence of microglia (Supplementary Figure 8). Kruskal-Wallis test with Dunn's post hoc test,  $H(3) = 54.74$ . Data are represented as mean  $\pm$  SEM from at least five independent experiments ( $n > 85$  for each group), p-values ranged from  $<0.001$  to 0.05, mg = microglia. (F) Representative images taken at 63x magnification using confocal microscopy of LAMP1 and SYN1 co-localization in IBA1 positive microglia as indicated by white arrow heads. A 3D stack of confocal images after IBA1 staining for microglia served as a mask to identify co-localizing endosomal LAMP1/SYN1 structures. Scale bar 20  $\mu$ m. (G) Change in mean fluorescence intensity of SYN1 within IBA1 positive microglia was analyzed for quantification of active presynaptic uptake by microglia. Kruskal-Wallis test with Dunn's post hoc test,  $H(3) = 96.1$ . Data are normalized to CTR microglia (mgCTR) cultured on CTR neurons and are represented as mean  $\pm$  SEM from at least five independent experiments ( $n > 125$  for each group), p-values ranged from  $<0.0001$  to 0.0135. (H) Microglial activation as quantified by the change of mean IBA1 fluorescence intensity of microglia after co-culture. Kruskal-Wallis test with Dunn's post hoc test,  $H(3) = 79.5$ . Data are normalized to CTR microglia (mgCTR) cultured on CTR neurons and are represented as mean  $\pm$  SEM from at least five independent experiments ( $n > 125$  for each group), p-values ranged from  $<0.001$  to 0.0014.

**Figure 6**

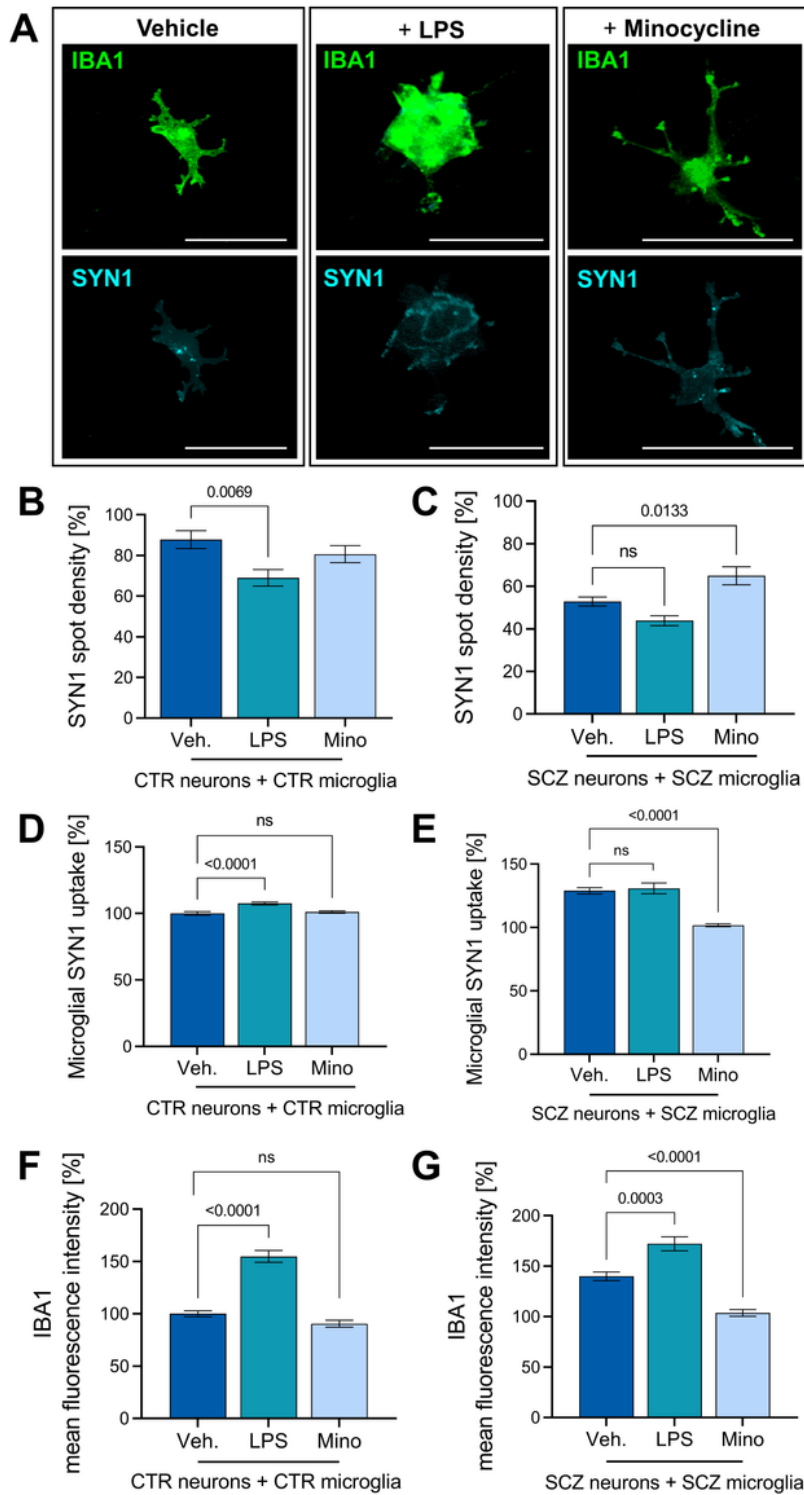


**Figure 6**

Anti-inflammatory pretreatment of microglia inhibits aberrant presynaptic uptake in SCZ patient-derived microglia. (A) Representative images taken at 63x magnification using confocal microscopy of immunocytochemical staining of SYN1 positive structures within IBA1 positive microglia after LPS (100 ng/ml) or minocycline (10  $\mu$ M) treatment. Scale bar 20  $\mu$ m. (B) Quantification of SYN1 spots in control cultures after co-culture with pretreated microglia. SYN1 spot densities were quantified on MAP2-positive

neuronal networks. Kruskal-Wallis test with Dunn's post hoc test,  $H(2) = 9.93$ ,  $p = 0.0069$ . Data are represented as mean  $\pm$  SEM from at least five independent experiments ( $n > 50$  for each treatment). (C) Quantification of SYN1 spots on SCZ neurons exposed to pretreated SCZ microglia. Kruskal-Wallis test with Dunn's post hoc test,  $H(2) = 15.0$ ,  $p = 0.0133$ . Data are represented as mean  $\pm$  SEM from at least five independent experiments ( $n > 59$  for each treatment). (D) Analysis of SYN1 uptake by pretreated IBA1-positive CTR-microglia after co-culture with CTR-neurons. SYN1 intensity was quantified in IBA1-positive masks. Kruskal-Wallis test with Dunn's post hoc test,  $H(2) = 35.76$ ,  $p < 0.0001$ . Data are represented as mean  $\pm$  SEM from at least five independent experiments ( $n > 86$  for each treatment). (E) Analysis of the mean SYN1 fluorescence intensity within pretreated IBA1 positive SCZ-microglia after co-culture with SCZ-neurons. Kruskal-Wallis test with Dunn's post hoc test,  $H(2) = 68.16$ ,  $p < 0.0001$ . Data are represented as mean  $\pm$  SEM from at least five independent experiments ( $n > 85$  for each treatment). (F) Microglial activation as determined by quantification of mean IBA1 fluorescence intensity of pretreated CTR-microglia after co-culture with CTR-neurons. Kruskal-Wallis test with Dunn's post hoc test,  $H(2) = 95.89$ ,  $p < 0.0001$ . Data are represented as mean  $\pm$  SEM from at least five independent experiments ( $n > 86$  for each treatment). (G) Microglial activation as determined by quantification of mean IBA1 fluorescence intensity of pretreated SCZ-microglia after co-culture with SCZ-neurons. Kruskal-Wallis test with Dunn's post hoc test,  $H(2) = 70.22$ ,  $p < 0.0001$  and  $p = 0.0003$ . Data are represented as mean  $\pm$  SEM from at least five independent experiments ( $n > 85$  for each treatment).

## Supplementary Files

This is a list of supplementary files associated with this preprint. Click to download.

- [SupplementaryInformation.docx](#)